

# Coarse-to-Fine Personalized LLM Impressions for Streamlined Radiology Reports

Chengbo Sun <sup>\*1</sup> Hui Yi Leong <sup>\*1</sup> Lei Li <sup>2</sup>

## Abstract

The manual creation of the "Impression" section in radiology reports is a primary driver of radiologist burnout. To address this, we propose a coarse-to-fine framework that uses open-source Large Language Models (LLMs) to automatically generate and personalize impressions from clinical findings. The system first generates a draft and then refines it using machine learning and Reinforcement Learning from Human Feedback (RLHF) to match individual radiologists' styles and ensure factual accuracy. We will fine-tune LLaMA and Mistral models on a large dataset of reports from the University of Chicago Medicine. Our approach aims to significantly reduce administrative workload and enhance reporting workflows while maintaining high standards of clinical precision.

## 1. Introduction

This research explores the application of large language models (LLMs) (Li et al., 2025; Cai et al., 2024; Yao et al., 2025) to a broader range of domains. Specifically, we investigate their use in summarizing radiology reports, addressing critical challenges in clinical decision-making and workflow efficiency. Artificial Intelligence (AI) and Natural Language Processing (NLP) have become integral to healthcare, enabling advancements in patient care, clinical workflows, and medical research. Applications include automating clinical documentation, such as extracting information from clinical notes or summarizing patient histories, as demonstrated in this research. These tools also enhance clinical decision support systems, improving the overall clinical experience.

Radiology reports are vital for clinical decision-making; however, generating personalized impressions is a time-

<sup>\*</sup>Equal contribution <sup>1</sup>University of Chicago <sup>2</sup>University of Washington. Correspondence to: Chengbo Sun, Hui Yi Leong, Lei Li <chengbo1@uchicago.edu, yuki.leong@uchicago.edu, lenny.lilei.cs@gmail.com>.

*Proceedings of the ICML 2025 Workshop on NewInML, Vancouver, Canada.*

### Background:

Male, 67 years old, with known right ICA plaque and area of right-sided ischemia on CT, evaluate for ischemia.

### Findings:

Patchy restricted diffusion is seen in the right centrum semiovale, along the right lateral ventricular atrium, within the right occipital lobe, and minimally in the right temporal lobe. These lesions demonstrate correlating T2 hyperintensity. A few additional scattered T2 hyperintense lesions are demonstrated in the cerebral hemispheres which do not show diffusion restriction. Evidence of a small chronic lacunar infarct is seen in the left basal ganglia, along with a small chronic right cerebellar cortical stroke. No evidence of significant generalized mass effect is seen. No acute intracranial hemorrhage or any abnormal extra-axial fluid collections are detected. The ventricles are normal in size and morphology.

### Impression:

1. Scattered areas of acute ischemia are seen within the right cerebral hemisphere, predominantly within the MCA distribution. 2. No evidence of significant generalized mass effect is seen. No intracranial hemorrhage is detected.

Figure 1. An example of background, finding, and impression.

intensive task that places a significant burden on radiologists. Radiologists routinely document findings from modalities such as X-rays, CT scans, MRIs, and ultrasounds in free text (Gundogdu et al., 2021). The Impression section, serving as the core summary, is critical for guiding referring physicians in their decisions. However, crafting impressions is inherently complex and demands a high level of personalization due to the integration of diverse medical data sources and patient-specific requirements. Additionally, the use of domain-specific language, as shown in Figure 1, further adds to the complexity, requiring deep expertise and precision.

Time constraints further exacerbate this challenge, as radiologists often work under tight schedules, leaving limited time to create detailed and personalized reports. Human-written impressions are prone to inefficiencies, errors, and overlooked details. Variability in style, structure, and thoroughness between healthcare providers can lead to discrepancies in report quality, affecting clinical outcomes. Digital tools are increasingly being developed to alleviate this administrative burden, allowing clinicians to focus more on patient care. However, existing LLMs often fail to meet the stylistic and clinical precision required for radiological impressions, highlighting the need for novel techniques to achieve fine-grained personalization.

---

General-purpose LLMs (Shi et al., 2025; Cai et al., 2025) are trained on broad datasets that lack the specialized vocabulary, style, and clinical nuances needed for medical reporting. They often cannot adapt their outputs to patient-specific needs or the unique preferences of individual practitioners or institutions (Yan et al., 2022). Additionally, these models struggle with maintaining fine-grained control over content and structure, making it difficult to ensure a consistent tone and alignment with input data. Such limitations can lead to trust issues in critical medical contexts.

This research introduces a novel approach to overcoming these challenges by proposing the Coarse-to-Fine generation framework. This framework bridges the gap between generic text generation and the stylistic and clinical precision required for medical imaging reports. It begins with a coarse-grained summary of the findings, capturing essential information from the input data. The outputs are then iteratively refined through fine-grained customization, incorporating patient-specific context, clinical precision, and stylistic alignment with medical standards. Finally, reinforcement learning with human feedback (RLHF) is applied to ensure the outputs are accurate and tailored to the needs of both clinicians and patients.

Our three main contributions are:

1. Propose a Coarse-to-Fine generation framework that combines high accuracy summarization with fine-grained personalization and aligns output with clinical and stylistic standards.
2. Construct and validate a multimodal dataset for personalized patient generation, ensuring the dataset captures diverse patient scenarios and aligns with real-world clinical requirements, enabling robust training and evaluation.
3. Achieve significant improvements in factual consistency, stylistic alignment, and personalization compared to baseline methods.

## 2. Related Work

### 2.1. Domain-Specific Pretrained Models in Biomedical and Clinical NLP

Early work in clinical NLP successfully adapted language models by pretraining them on domain-specific corpora. This trend began with models like BioBERT (Lee et al., 2020) on biomedical literature and was extended by BlueBERT (Peng et al., 2020) and ClinicalBERT (Alsentzer et al., 2019) using clinical notes from EMRs. These models set new benchmarks on discriminative tasks like named entity recognition (NER) and relation extraction. The approach was further specialized for radiology with RadBERT (Yan

et al., 2022), which was pretrained on millions of radiology reports for tasks like report coding and summarization. However, a key limitation of these BERT-based, encoder-only architectures is their restricted performance on complex natural language generation (NLG) tasks, which is the primary focus of our work.

### 2.2. Foundational models and applications

The advent of modern foundational LLMs has opened new possibilities for high-quality text generation. However, these models present distinct trade-offs for clinical applications, as summarized in Table 1. For example, Mistral-7b (Jiang et al., 2023) is optimized for inference efficiency, while Gemma models (Team et al., 2024) are designed for efficient domain adaptation. While proprietary models like GPT-4o (Achiam et al., 2023) offer exceptional performance, their closed nature limits customization for specific clinical workflows. In contrast, open-source models like Llama-3.1-8B (Dubey et al., 2024) provide a strong balance, supporting long context windows of up to 128K tokens suitable for extensive radiology reports. Given these factors and its superior performance in our preliminary evaluations (Section 5.2), we selected Llama-3.1-8b as the base for our framework.

### 2.3. LLM and framework in healthcare

In the healthcare domain, large language models have first been fine-tuned to generate structured SOAP notes, as demonstrated by Leong et al.’s efficient fine-tuning approach (Leong et al., 2024b). Building on this work, MediNote is the first end-to-end generative AI framework that combines retrieval-augmented generation (RAG), parameter-efficient fine-tuning, and ambient listening to convert raw clinical conversations directly into SOAP documentation (Leong et al., 2024a). Complementing these advances, AgentNet (Leong & Wu, 2024) and (Wang et al., 2025) employs a fully decentralized, retrieval-augmented architecture in which autonomous agents dynamically reconfigure their roles and interconnections within a directed acyclic graph to optimize clinical workflows and improve patient outcomes in healthcare. Together, these developments chart a clear progression—from LLM fine-tuning for note generation, through RAG-enhanced generative frameworks, to autonomous multi-agent systems—highlighting the evolving landscape of AI-driven healthcare solutions.

## 3. Data exploration

The data we use are the 957,134 de-identified radiology reports obtained from the University of Chicago (UC) Medicine (Gundogdu et al., 2021), curated over the last 12 years until January 1st, 2020. The dataset presented is a collection of radiology reports structured for clinical sum-

Table 1. Existing LLM methods for Summarization.

METHOD	ADVANTAGES	DISADVANTAGES
GEMMA-2-9B (TEAM ET AL., 2024)	OFFERS A TRADE-OFF BETWEEN MODEL SIZE AND TASK EFFICIENCY, SUITABLE FOR DIVERSE NLP TASKS.	PERFORMANCE LAG BEHIND MORE ADVANCED MODELS LIKE LLAMA 3.1 OR GPT-4 IN COMPLEX REASONING TASKS.
MISTRAL-7B (JIANG ET AL., 2023)	EFFECTIVE FOR HANDLING LARGE DATASETS AND EXTENDED SEQUENCES WITH MINIMAL LATENCY	REQUIRES ADDITIONAL FINE-TUNING FOR DOMAIN-SPECIFIC TASKS LIKE RADIOLogy SUMMARIZATION.
GPT-4O (ACHIAM ET AL., 2023)	EXCELS IN UNDERSTANDING, SUMMARIZING, AND REASONING, OUTPERFORMING MOST OPEN-SOURCE MODELS.	ACCESS REQUIRES A SUBSCRIPTION, AND FINE-TUNING IS OFTEN LIMITED OR EXPENSIVE (JIANG ET AL., 2024).
LLAMA-3.1-8B (DUBEY ET AL., 2024)	SUPPORTS CONTEXT WINDOWS OF UP TO 128K TOKENS, SUITABLE FOR PROCESSING EXTENSIVE RADIOLOGY REPORTS. OPTIMIZED FOR FEWER TRAINING SAMPLES, REDUCING COMPUTATIONAL COSTS.	DESPITE ITS OPTIMIZATIONS, FINE-TUNING AND DEPLOYMENT MAY STILL DEMAND SIGNIFICANT RESOURCES.

marization tasks, making it highly suitable for fine-tuning large language models (LLMs) in the medical domain. It is organized into three primary columns: *clinical information*, *findings*, and *impression*. The clinical information column provides a brief overview of the patient’s medical history and the reason for the radiological examination. The findings column contains detailed imaging observations, while the impression column provides a concise diagnostic summary based on the findings. This structure creates a clear alignment between input (findings) and target output (impression), which is ideal for supervised summarization tasks.

A random sampling of 7,893 reports was analyzed, with an average token count of 123 and a total of approximately

97 million tokens. The Info/Impression Token Count Ratio highlights the difference in length between findings and impressions, with a mean ratio of 7.57, emphasizing the challenge of generating highly concise summaries from more detailed observations.

From a natural language processing (NLP) perspective, the dataset is well-suited for sequence-to-sequence tasks due to its consistent structure and domain specificity. The hierarchical nature of the data—where detailed multi-level observations in the findings are summarized into condensed impressions—poses a unique challenge for LLMs, requiring both factual accuracy and syntactic fluency. The length asymmetry between the findings and impressions adds complexity, as models must process long-context inputs while generating concise outputs without losing critical information.

## 4. Methodology

### 4.1. Overview

In this study, we propose a systematic approach to evaluate and fine-tune large language models (LLMs) for the task of radiology findings summarization. The methodology is divided into three main stages: Model Selection, Evaluation, and Radiology Expert Study, as illustrated in the architecture diagram Figure 2.

The proposed method leverages a coarse-to-fine generation approach to automate the creation of radiological impressions, incorporating a dual-stage pipeline for preliminary and refined outputs. The system begins with data preparation for classification. The summarization is performed using the Llama 8B model, which generates the impressions. The generated results are evaluated based on ROUGE scores, BLUE scores, BERT scores and factual consistency.

Once the results are deemed acceptable, they are customized using engineered prompts tailored to three target audiences:

1. Brief Summarization: Simplified summaries designed for non-English speakers.
2. Bullet Point Summarization: Summaries with clear, concise insights for quick review.
3. Comprehensive Summarization: Detailed summaries aimed at experts.

This customized output is designed for diverse clinical interactions, enhancing its applicability across various healthcare scenarios. The proposed methodology ensures accuracy and adaptability, making it a valuable tool for radiology workflows.

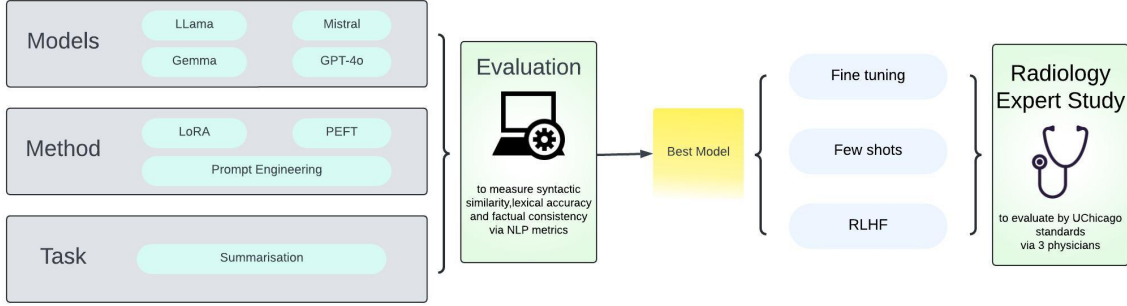


**Figure 2. Architecture Overview:** This architecture outlines the process used for clinical report summarization and evaluation. Multiple large language models (LLMs), including LLaMA, Gemma, Mistral, and GPT-4o, were tested using different methods such as LoRA and PEFT for parameter-efficient fine-tuning, alongside prompt engineering strategies. The models were evaluated on metrics like syntactic similarity, lexical accuracy, and factual consistency to identify the best-performing model. After model selection, further fine-tuning and few-shot learning were applied, followed by reinforcement learning with human feedback (RLHF). Finally, a radiology expert study, conducted by three physicians following UChicago standards, validated the clinical relevance and accuracy of the generated summaries.

**Table 2. Summary Performance Metrics Averaged Over 10 Radiology Reports**

MODEL	ROUGE	BLUE	BERT	FC
GEMMA-2-9B	0.368	0.032	1.78	0.58
MISTRAL-7B	0.371	0.031	1.76	<b>0.69</b>
LLAMA-3.1-8B	<b>0.385</b>	<b>0.037</b>	<b>1.78</b>	0.68

#### 4.2. Model selection

**Evaluation** The models were evaluated on a randomly selected subset of 10 radiology findings from the University of Chicago Radiology Report Dataset, ensuring the task’s relevance to clinical workflows. The following metrics were used to measure performance:

- ROUGE: We applied ROUGE-1, ROUGE-2 and ROUGE-L to quantify syntactic similarity between generated and reference impression, capturing overlapping words and phrases. Formally, ROUGE-N is an n-gram recall between a candidate summary and a set of reference impressions (Lin, 2004). ROUGE-N is computed as follows:

$$\text{ROUGE-N} = \frac{\sum_{S \in \{\text{Ref}\}} \sum_{\text{gram}_n \in S} \text{Count}_{\text{match}}(\text{gram}_n)}{\sum_{S \in \{\text{Ref}\}} \sum_{\text{gram}_n \in S} \text{Count}(\text{gram}_n)} \quad (1)$$

Where  $n$  stands for the length of the n-gram, gramm, and Countmatch(gramm) is the maximum number of n-grams co-occurring in a generated summary and reference impression. We propose using the longest common subsequence LCS-based Fmeasure to estimate the similarity between generated summary  $X$  of length  $m$  and reference impression  $Y$  of length  $n$ , assuming  $X$  is a reference summary sentence and  $Y$  is a candidate

summary sentence, as follows:

$$R_{\text{LCS}} = \frac{\text{LCS}(X, Y)}{m} \quad (2)$$

$$P_{\text{LCS}} = \frac{\text{LCS}(X, Y)}{n} \quad (3)$$

$$F_{\text{LCS}} = \frac{(1 + b^2)R_{\text{LCS}}P_{\text{LCS}}}{R_{\text{LCS}} + b^2P_{\text{LCS}}} \quad (4)$$

Where  $\text{LCS}(X, Y)$  is the length of a longest common subsequence of  $X$  and  $Y$ . We call the LCS-based F-measure, i.e. Equation 4, ROUGE-L.

- BLEU (Papineni et al., 2002): Evaluates lexical accuracy by comparing generated summary n-gram overlap with the reference impression. We first compute the geometric average of the generated summary n-gram precisions,  $p_m$  which is the same Equation 1 using generated summary n-grams up to length  $M$  and positive weights  $w_m$  summing to one. Next, let  $c$  be the length of the candidate translation and  $r$  be the effective reference corpus length. We compute the brevity penalty  $BP$ ,

$$BP = \begin{cases} 1 & \text{if } c > r, \\ e^{(1-r/c)} & \text{if } c \leq r. \end{cases} \quad (5)$$

Then,

$$\text{BLEU} = BP \cdot \exp \left( \sum_{m=1}^M w_m \log p_m \right) \quad (6)$$

- BERTScore (Zhang et al., 2020): Assesses semantic similarity by comparing embeddings of generated

and reference texts, focusing on meaning preservation. We use the tokenizer provided with our model. Given a tokenized reference impression sentence  $x = \langle x_1, \dots, x_k \rangle$ , the embedding model generates a sequence of vectors  $\langle \mathbf{x}_1, \dots, \mathbf{x}_k \rangle$ . Similarly, the tokenized generated summary  $\hat{x} = \langle \hat{x}_1, \dots, \hat{x}_m \rangle$  is mapped to  $\langle \hat{\mathbf{x}}_1, \dots, \hat{\mathbf{x}}_m \rangle$ . The cosine similarity of a reference impression token  $x_i$  and a generated summary token  $\hat{x}_j$  is  $\frac{\mathbf{x}_i^\top \hat{\mathbf{x}}_j}{\|\mathbf{x}_i\| \|\hat{\mathbf{x}}_j\|}$ . We use pre-normalized vectors, which reduces this calculation to the inner product  $\mathbf{x}_i^\top \hat{\mathbf{x}}_j$ .

The complete score matches each token in  $x$  to a token in  $\hat{x}$  to compute recall, and each token in  $\hat{x}$  to a token in  $x$  to compute precision. We use greedy matching to maximize the matching similarity score, where each token is matched to the most similar token in the other sentence. We combine precision and recall to compute an F1 measure. For a reference  $x$  and candidate  $\hat{x}$ , the recall, precision, and F1 scores are:

$$R_{\text{BERT}} = \frac{1}{|x|} \sum_{x_i \in x} \max_{\hat{x}_j \in \hat{x}} x_i^\top \hat{x}_j \quad (7)$$

$$P_{\text{BERT}} = \frac{1}{|\hat{x}|} \sum_{\hat{x}_j \in \hat{x}} \max_{x_i \in x} x_i^\top \hat{x}_j \quad (8)$$

$$F_{\text{BERT}} = \frac{2 \cdot P_{\text{BERT}} \cdot R_{\text{BERT}}}{P_{\text{BERT}} + R_{\text{BERT}}} \quad (9)$$

- **Factual Consistency (FC)(Kryściński et al., 2019):** Measures alignment between generated summaries and input findings to ensure the generated output accurately reflects the clinical observations. To evaluate the factual consistency of our model-generated summaries, we applied the TrueTeacher-based T5-11B model(Gekhman et al., 2023), which was fine-tuned on ANLI and TrueTeacher data. This model was used as a factual evaluator to compare generated summaries against the original findings from radiology reports. We framed the task as a Natural Language Inference (NLI) problem, where the generated summary served as the hypothesis and the original findings as the premise. The model provided entailment probabilities that indicated the degree of factual consistency, offering a quantitative measure of how accurately the generated summary preserved the key information from the original findings. This methodology allowed for robust, scalable evaluation of factual consistency in a domain-specific context.

Each metric highlights different aspects of summarization: syntax, semantics, lexical accuracy, and factual consistency. Together, they provide a holistic view of model performance.

As shown in Table 2, Llama-3.1-8b consistently outperformed the other models across all metrics. It achieved the highest ROUGE score of 0.385, indicating superior overlap between its generated summaries and the ground truth impressions. Its BLEU score of 0.037 demonstrates better word-level precision compared to Gemma-2-9b and Mistral-7b. The BERTScore of 1.78 further highlights Llama-3.1-8b’s contextual and semantic alignment with the reference summaries, showcasing its ability to capture nuanced medical terminology.

In addition to linguistic quality, factual consistency is critical for radiology findings summarization. Mistral-7b achieved a factual consistency score of 0.69, narrowly outperforming Llama-3.1-8b at 0.68. Despite this minor difference, Llama-3.1-8b provided the most balanced performance across all metrics, demonstrating its robustness in handling radiology-specific language and maintaining factual integrity.

Our results confirm that Llama-3.1-8b is the most suitable choice for radiology findings summarization due to its superior linguistic quality, semantic understanding, and balanced factual consistency. These results underscore the model’s capability to address the unique challenges of medical summarization tasks, such as handling domain-specific terminology and ensuring clinical relevance.

*Best Model Selection and Fine-Tuning* Based on the evaluation, LLaMA-3.1-8b emerged as the best model, achieving the highest ROUGE, BLEU, and BERTScore, with a factual consistency score of 0.68. This model was further optimized through:

**Fine-Tuning:** The model was trained on additional domain-specific radiology datasets to align with clinical language and terminology. **Few-Shot Learning:** Leveraging few-shot prompts, the model was fine-tuned to generalize effectively with minimal examples. **Reinforcement Learning with Human Feedback (RLHF):** Incorporating feedback from radiologists to refine the generated summaries, ensuring clinical relevance and coherence. These techniques improved the model’s ability to generate summaries that are both accurate and clinically useful.

### 4.3. Model Training and Fine-tuning

The proposed approach utilizes a parameter-efficient fine-tuning (PEFT) technique implemented with the FastLanguageModel library(Xu et al., 2023). The base model is optimized using Low-Rank Adaptation (LoRA)(Hao et al., 2024), a strategy that adds trainable low-rank matrices to specific layers of the model, enabling efficient adaptation to new tasks with minimal computational overhead. We fine-tuned the base model using parameter-efficient fine-tuning (PEFT) with LoRA, implemented via the FastLanguageModel library. A rank of 16 was chosen to balance efficiency

and performance, with adapters applied to core transformer modules. LoRA alpha was set to 16, with dropout disabled to fully utilize gradient updates. Bias was set to "none" to reduce parameter overhead. Gradient checkpointing with UnsLoft reduced VRAM usage by 30%, enabling longer sequences and larger batch sizes. A fixed random seed (3407) ensured reproducibility. While options like LoftQ and RSLora were not used, they remain viable for future optimization. The model is fine-tuned using Supervised Fine-Tuning (SFT) with the `SFTTrainer` class, a robust and flexible framework for adapting large language models to custom datasets. The fine-tuning process begins with data preparation, where the training dataset is preprocessed to ensure proper tokenization and sequence length adjustment. Long sequences are truncated to fit the model's maximum sequence length, and the `text` field of the dataset is used for training inputs. During training, the batch size is set to 1 per device, with gradient accumulation steps configured as 2 to effectively simulate a batch size of 2. Training is conducted over 50 epochs with a maximum of 60 gradient updates, balancing computational cost and fine-tuning depth. A linear learning rate scheduler is applied, starting at 1e-4, with 5 warmup steps to stabilize the optimization process. Mixed-precision training, leveraging FP16 or BF16 precision based on hardware support, is employed to improve computational efficiency. The AdamW optimizer with 8-bit precision (`adamw_8bit`) reduces memory requirements while maintaining performance, and a weight decay of 0.01 is used to prevent overfitting. Logging occurs at every step to monitor progress, and all outputs are stored in the `outputs` directory for subsequent evaluation. To streamline the training process, external reporting tools such as WandB are disabled. This fine-tuning strategy integrates the parameter efficiency of LoRA and the scalability of the `SFTTrainer`, enabling the adaptation of pre-trained large language models to domain-specific tasks while minimizing computational and memory overhead. The approach ensures optimal model performance on limited hardware resources, making it suitable for real-world applications.

#### 4.4. Coarse-to-Fine Generation Process

The Coarse Stage initiates the summarization process by utilizing large language models (LLMs) to generate preliminary impressions based on the input findings and patient data. This stage is designed to capture primary clinical insights while ensuring the output follows a structured format. We designed a prompt engineering strategy that evolves from a simple base prompt to more detailed and customized versions tailored for specific audiences. The base model utilizes a straightforward prompt, such as "Summarize the following input" (Wang et al., 2023), which generates bullet-point key points. Building on this, we incorporated role descriptions and task-specific instructions

to produce more detailed outputs while maintaining the bullet-point structure. Additionally, we provided three-shot examples to guide the model in generating outputs aligned with specific writing styles and standards. For expert-level outputs, the prompts further emphasize role descriptions, expanded task instructions, and a clear definition of the target audience to ensure the generated content meets their expectations. Users can also adjust the output length based on specific requirements. Full details of the prompts, including examples for base, detailed, and expert versions, are provided in Figure 3.

This structured progression not only improves the quality of the generated outputs but also enhances the model's ability to adapt to varying user requirements, ensuring consistency and precision. The flow chart visually encapsulates this iterative and hierarchical prompt engineering strategy, emphasizing the systematic refinement process.

## 5. Experiment

### 5.1. Experiment setup

For our experiments, we curated a training set of 500 reports from the University of Chicago dataset, balanced and stratified by patient gender and age. An additional 50 reports were held out for testing. Our model was fine-tuned using a parameter-efficient approach (PEFT) with Low-Rank Adaptation (LoRA), setting the rank to 16 and alpha to 16. We utilized the `SFTTrainer` with a batch size of 2 (1 per device with 2 gradient accumulation steps), the AdamW 8-bit optimizer, and a linear learning rate scheduler starting at 1e-4. The model was trained for up to 50 epochs on a single Google T4 GPU, a process which took less than 25 minutes. All evaluation was performed using the metrics detailed in Section 4.2. An exhaustive list of all hyperparameters can be found in the appendix.

### 5.2. Comparison experiments.

Table 3. Summary Performance Metrics Averaged Over 10 Radiology Reports

MODEL	ROUGE	BLUE	BERT	FC
GEMMA-2-9B	0.368	0.032	1.78	0.58
MISTRAL-7B	0.371	0.031	1.76	<b>0.69</b>
LLAMA-3.1-8B	0.385	0.037	1.78	0.68
CORSE2FINE	<b>0.420</b>	<b>0.041</b>	<b>2.51</b>	0.612

*Output results* We introduced a style-conditioning mechanism that allows the model to generate impressions tailored to user preferences, ranging from concise summaries to more elaborate outputs. Examples of the results are shown in Figure 4. The original finding was notably long, but aside from highlighting the key disease, as shown in Figure 4, it

Basic prompt	<i>Summarize the following input</i>
Prime prompt	<i>You are a [Role description]. You can summarize medical reports based on the findings</i>
Expert prompt	<i>You are a [Expert role description]. Your [Task description] and produce [Impression requirements' details]. This summary should be [Expert requirements] for a [Expert user descriptions].</i>
Plain prompt	<i>You are a [Expert role description]. Your [Task description] and write [Plain English impression requirements]. Focus on [Most important points] in short, easy, plain English for [Non-English user descriptions].</i>

Figure 3. Prompts examples

also included information on 10 additional examinations, all of which were either negative or unchanged. Consequently, the generated impression summarized these findings as "Stable examination."

Our model demonstrated the ability to accurately summarize the relevant disease while appropriately disregarding the negative or unchanged results. This highlights the model's effectiveness in prioritizing clinically significant information and producing concise, context-appropriate impressions, improving both efficiency and clarity for end users.

The highlighted sections in the findings represent the most important details. These key points were successfully captured and summarized in all versions of the generated outputs, with accurate and contextually appropriate descriptions.

To address this limitation, we conducted human assessments involving one radiologist from UC Medicine and an independent external board-certified radiologist.

We randomly selected 300 reports from the UC Medicine test set, consisting of 200 generated by our fine-tuned model and 100 original reports, randomly mixed. Radiologists compared the predicted impressions with the original ones, assigning one of three ratings: 'positive' if the model-generated impression was preferred, 'negative' if the original impression was deemed superior, and 'neutral' if both were equally accurate. The figure 5 illustrates the average rating scores across five dimensions: Clearance, Completeness, Human-likeness, Conciseness, and Coherence. Notably, 'positive' ratings were frequently given when the model successfully captured incidental findings that were omitted in the original impressions.

Out of the 200 generated reports, 145 were labeled as "neutral," 14 as "positive," and 30 as "negative." Eleven reports were excluded due to unresolved discrepancies between the evaluators, leaving 289 reports for the final analysis. Overall, 79.5% of the evaluated samples received either "neutral" or "positive" votes, indicating that the majority of the system's predictions were considered by radiologists to be at least as accurate as human-generated impressions.

*Stability test* To evaluate robustness against real-world data entry errors, we tested our model on findings with a simulated 3% typographical error rate. The model's performance remained remarkably stable, showing only minimal degradation compared to the clean dataset (ROUGE: 0.370, BERT: 2.49). This resilience to noisy input highlights its reliability for practical clinical applications.

*Universality test* To test the generalizability of our model, we applied it to the external CheXpert Plus dataset. As shown in the example in Figure 6, the model effectively summarized key clinical findings even with a different data source and writing style. In a review of 10 reports from this dataset, radiologists rated the generated impressions as equal to or better than the original in 80% of cases (3 positive, 5 neutral, 2 negative), demonstrating the model's strong versatility.

Besides, 10 results haven been reviewed by our radiologist, 3 reports are marked positive, 5 reports are marked natural and 2 are marked negative. the results show our model's strong versatility for other institution's dataset or writing styles.

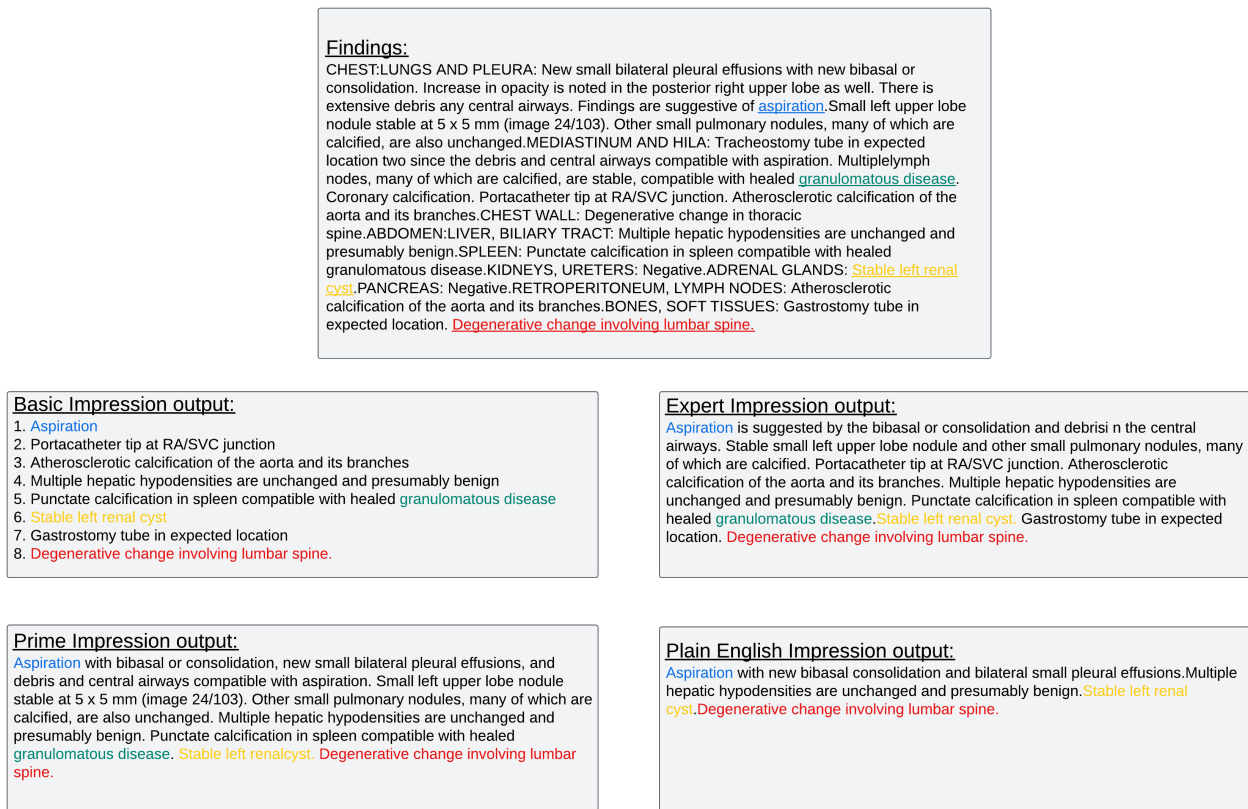


Figure 4. Findings and generated impression examples

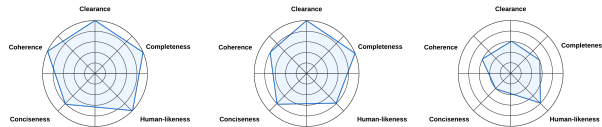


Figure 5. **Hexagon Rating:** From left to right are the positive rating, neutral rating, and negative rating respectively, illustrating the average rating scores for the 200 generated reports. The pentagon visualizes five key dimensions of summary quality: Clearance, Completeness, Human-likeness, Conciseness, and Coherence. Higher values along each axis indicate better performance in the corresponding metric.

## 6. Conclusion

In this paper, we presented a Coarse-to-Fine Personalized LLM framework for generating streamlined radiology impressions. Our approach leverages open-source models and parameter-efficient fine-tuning techniques, such as LoRA, to generate clinically relevant, stylistically aligned summaries. Through a two-stage generation process—beginning with coarse summaries and refined via prompt engineering and

reinforcement learning with human feedback (RLHF)—the system adapts to diverse clinical needs. Experiments on the University of Chicago dataset demonstrated improvements in factual consistency, linguistic quality, and expert preference ratings. Stability and generalizability were further validated through robustness testing and application to the CheXpert Plus dataset. Looking ahead, we aim to integrate visual data and explore advanced multi-modal models to enhance clinical reasoning and support real-world diagnostic workflows.

## References

Achiam, J., Adler, S., Agarwal, S., Ahmad, L., Akkaya, I., Aleman, F. L., Almeida, D., Altenschmidt, J., Altman, S., Anadkat, S., et al. Gpt-4 technical report. *arXiv preprint arXiv:2303.08774*, 2023.

Alsentzer, E., Murphy, J. R., Boag, W., Weng, W.-H., Jin, D., Naumann, T., and McDermott, M. Publicly available clinical bert embeddings. *arXiv preprint arXiv:1904.03323*, 2019.

Cai, C., Zhao, X., Liu, H., Jiang, Z., Zhang, T., Wu, Z.,

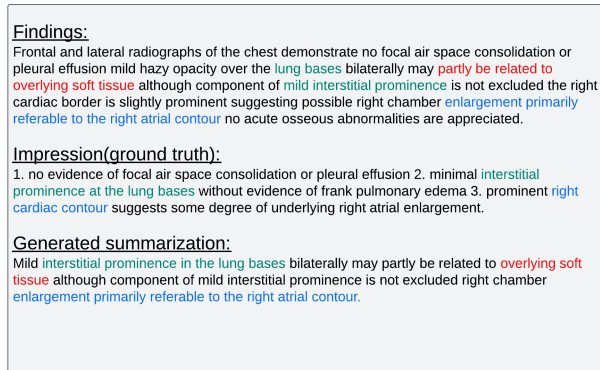


Figure 6. Generated result example of CheXpert Plus dataset

Hwang, J.-N., Belongie, S., and Li, L. The role of deductive and inductive reasoning in large language models. *arXiv preprint arXiv:2410.02892*, 2024.

Cai, C., Liu, H., Zhao, X., Jiang, Z., Zhang, T., Wu, Z., Lee, J., Hwang, J.-N., and Li, L. Bayesian optimization for controlled image editing via llms. *arXiv preprint arXiv:2502.18116*, 2025.

Dubey, A., Jauhri, A., Pandey, A., Kadian, A., Al-Dahle, A., Letman, A., Mathur, A., Schelten, A., Yang, A., Fan, A., et al. The llama 3 herd of models. *arXiv preprint arXiv:2407.21783*, 2024.

Gekhman, Z., Herzig, J., Aharoni, R., Elkind, C., and Szpektor, I. Trueteacher: Learning factual consistency evaluation with large language models, 2023.

Gundogdu, B., Pamuksuz, U., Chung, J. H., Telleria, J. M., Liu, P., Khan, F., and Chang, P. J. Customized impression prediction from radiology reports using bert and lstm s. *IEEE Transactions on Artificial Intelligence*, 4(4):744–753, 2021.

Hao, Y., Cao, Y., and Mou, L. Flora: Low-rank adapters are secretly gradient compressors. *arXiv preprint arXiv:2402.03293*, 2024.

Jiang, A. Q., Sablayrolles, A., Mensch, A., Bamford, C., Chaplot, D. S., Casas, D. d. l., Bressand, F., Lengyel, G., Lample, G., Saulnier, L., et al. Mistral 7b. *arXiv preprint arXiv:2310.06825*, 2023.

Jiang, Y., Chen, C., Nguyen, D., Mervak, B. M., and Tan, C. Gpt-4v cannot generate radiology reports yet. *arXiv preprint arXiv:2407.12176*, 2024.

Kryściński, W., McCann, B., Xiong, C., and Socher, R. Evaluating the factual consistency of abstractive text summarization. *arXiv preprint arXiv:1910.12840*, 2019.

Lee, J., Yoon, W., Kim, S., Kim, D., Kim, S., So, C. H., and Kang, J. Biobert: a pre-trained biomedical language representation model for biomedical text mining. *Bioinformatics*, 36(4):1234–1240, 2020.

Leong, H. Y. and Wu, Y. Why should next-gen llm multi-agent systems move beyond fixed architectures to dynamic, input-driven graphs? SSRN Working Paper, 2024. URL <https://ssrn.com/abstract=5276004>.

Leong, H. Y., Gao, Y., and Ji, S. A gen ai framework for medical note generation. In *Proceedings of the 2024 6th International Conference on Artificial Intelligence and Computer Applications (ICAICA)*, pp. 423–429, 2024a. doi: 10.1109/ICAICA63239.2024.10823004.

Leong, H. Y., Gao, Y., Ji, S., Zhang, Y., and Pamuksuz, U. Efficient fine-tuning of large language models for automated medical documentation. In *Proceedings of the 2024 4th International Conference on Digital Society and Intelligent Systems (DSInS)*, pp. 204–209, Sydney, Australia, 2024b. doi: 10.1109/DSInS64146.2024.10992195.

Li, L., Jia, S., Wang, J., Jiang, Z., Zhou, F., Dai, J., Zhang, T., Wu, Z., and Hwang, J.-N. Human motion instruction tuning. In *Proceedings of the Computer Vision and Pattern Recognition Conference*, pp. 17582–17591, 2025.

Lin, C.-Y. ROUGE: A package for automatic evaluation of summaries. In *Text Summarization Branches Out*, pp. 74–81, Barcelona, Spain, July 2004. Association for Computational Linguistics. URL <https://aclanthology.org/W04-1013/>.

Papineni, K., Roukos, S., Ward, T., and Zhu, W.-J. Bleu: a method for automatic evaluation of machine translation. In *Annual Meeting of the Association for Computational Linguistics*, 2002. URL <https://api.semanticscholar.org/CorpusID:11080756>.

Peng, Y., Chen, Q., and Lu, Z. An empirical study of multi-task learning on bert for biomedical text mining. *arXiv preprint arXiv:2005.02799*, 2020.

Shi, J., Ma, Q., Liu, H., Zhao, H., Hwang, J.-N., and Li, L. Explaining context length scaling and bounds for language models. *arXiv preprint arXiv:2502.01481*, 2025.

Team, G., Mesnard, T., Hardin, C., Dadashi, R., Bhupatiraju, S., Pathak, S., Sifre, L., Rivière, M., Kale, M. S., Love, J., et al. Gemma: Open models based on gemini research and technology. *arXiv preprint arXiv:2403.08295*, 2024.

---

Wang, B., Li, Y., Zhou, Q., Leong, H. Y., Zhao, T., Ye, L., Deng, H., Luo, D., and Vasconcelos, N. One Image Growing Up: A knowledge-grounding evaluation framework for multimodal large language models' visual perspective-taking. In *Workshop on Assessing World Models: Methods and Metrics for Evaluating Understanding*, July 2025. URL <https://openreview.net/forum?id=iekoq1rv>. ICML 2025, Vancouver, Canada.

Wang, L., Xu, W., Lan, Y., Hu, Z., Lan, Y., Lee, R. K.-W., and Lim, E.-P. Plan-and-solve prompting: Improving zero-shot chain-of-thought reasoning by large language models. *arXiv preprint arXiv:2305.04091*, 2023.

Xu, L., Xie, H., Qin, S.-Z. J., Tao, X., and Wang, F. L. Parameter-efficient fine-tuning methods for pretrained language models: A critical review and assessment. *arXiv preprint arXiv:2312.12148*, 2023.

Yan, A., McAuley, J., Lu, X., Du, J., Chang, E. Y., Gentili, A., and Hsu, C.-N. Radbert: adapting transformer-based language models to radiology. *Radiology: Artificial Intelligence*, 4(4):e210258, 2022.

Yao, Z., Cheng, X., Huang, Z., and Li, L. Countllm: Towards generalizable repetitive action counting via large language model. In *Proceedings of the Computer Vision and Pattern Recognition Conference*, pp. 19143–19153, 2025.

Zhang, T., Kishore, V., Wu, F., Weinberger, K. Q., and Artzi, Y. Bertscore: Evaluating text generation with bert, 2020. URL <https://arxiv.org/abs/1904.09675>.